

# Composites of Single-Walled Carbon Nanotubes and Polystyrene: Preparation and Electrical Conductivity

Maxim N. Tchoul,<sup>†</sup> Warren T. Ford,<sup>\*,†</sup> Mai L. P. Ha,<sup>‡</sup> Israel Chavez-Sumarriva,<sup>‡</sup>  
Brian P. Grady,<sup>‡</sup> Giulio Lolli,<sup>‡</sup> Daniel E. Resasco, and Sivaram Arepalli<sup>§</sup>

Department of Chemistry, Oklahoma State University, 107 Physical Sciences I, Stillwater Oklahoma 74078, School of Chemical, Biological and Materials Engineering, University of Oklahoma, 100 East Boyd Street, Norman Oklahoma 73019; and ERC Incorporated/NASA Johnson Space Center, mail code ES4, 2101 NASA Parkway, Houston, Texas 77058

Received December 19, 2007. Revised Manuscript Received February 11, 2008

Composites of single-walled carbon nanotubes (SWNT) and polystyrene have been prepared using three different types of SWNT: HiPco, CoMoCat, and pulsed laser vaporization (PLV). Nanotubes were incorporated into the polystyrene matrix by two methods: (1) evaporation of chloroform solutions of SWNT noncovalently functionalized with poly[(m-phenylenevinylene)-co-(2,5-dioctoxy-p-phenylenevinylene)] (PmPV) and polystyrene; (2) coagulation in water of DMF solutions containing polystyrene and nitric acid oxidized SWNT. From measurements of the electrical conductivities of the composites over a range of concentration from 0.1 to 6 wt % SWNT, the percolation threshold of conductivity was 0.17–0.3% SWNT for the PmPV-coated materials and 0.4–0.5% for those made by coagulation. Of the three types of SWNT, composites made with HiPco tubes had the highest conductivity.

## Introduction

Carbon nanotubes possess high mechanical strength, high electrical and thermal conductivity, and unique optical and electronic properties.<sup>1</sup> These properties make carbon nanotubes valuable for a wide range of applications. Electrical conductivity of individual bundles of metallic carbon nanotubes reaches the value of  $10^4$  S/cm,<sup>2</sup> which is close to that of metals ( $59 \times 10^4$  S/cm for copper and  $9.9 \times 10^4$  S/cm for iron), even though the density of nanotubes is much lower. Thus carbon nanotubes are excellent candidates to blend with polymers to produce electrostatic dissipative materials and other useful components in electronics. However, the potentially superb properties of composites made with SWNT have not been achieved because of poor dispersion of the nanotubes. For example, a dispersion of individual nanotubes having an aspect ratio of 1000 theoretically has a percolation threshold of electrical conductivity at approximately 0.05 vol %.<sup>3</sup> The experimental conductivities of CNT–polymer composites have percolation thresholds ranging from 0.0025%<sup>5</sup> to several percent, depending on the

type of polymer and method of composite preparation. Values of 0.1–1% are most common.<sup>3–12</sup>

The conductivity of a composite  $\sigma$  vs volume fraction of nanotubes  $f$  follows the scaling law<sup>13</sup>

$$\sigma = C(f - f_c)^\beta \quad (1)$$

where  $f_c$  is the volume fraction at the percolation threshold and  $\beta$  and  $C$  are constants. Because the percolation threshold is greatly dependent on the spatial distribution of nanotubes in the polymer matrix,<sup>14,15</sup> it is possible to use this parameter to assess the quality of nanotube dispersion in composites. The basic approaches utilized for incorporation of nanotubes into the polymer matrix include melt mixing,<sup>9,10</sup> in situ polymerization,<sup>3,7</sup> and solution processing.<sup>6,8,12</sup> The latter two methods have given better results due to a more uniform distribution of nanotubes in a low-viscosity liquid phase that results in a more uniform mixing with polymer.

\* To whom correspondence should be addressed. E-mail: warren.ford@okstate.edu.

<sup>†</sup> Oklahoma State University.

<sup>‡</sup> University of Oklahoma.

<sup>§</sup> ERC Incorporated/NASA Johnson Space Center.

- (1) O'Connell, M. J., Ed. *Carbon Nanotubes: Properties and Applications*; CRC Press: Boca Raton, FL, 2006.
- (2) Thess, A.; Lee, R.; Nikolaev, P.; Dai, H.; Petit, P.; Robert, J.; Xu, C.; Lee, Y. H.; Kim, S. G.; Rinzler, A. G.; Colbert, D. T.; Scuseria, G. E.; Tomanek, D.; Fischer, J. E.; Smalley, R. E. *Science* **1996**, *273*, 483.
- (3) Ounaies, Z.; Park, C.; Wise, K. E.; Stiochi, E. J.; Harrison, J. S. *Compos. Sci. Technol.* **2003**, *63*, 1637.
- (4) Ramasubramaniam, R.; Chen, J. *Appl. Phys. Lett.* **2003**, *83*, 2928.
- (5) Sandler, J. K. W.; Kirk, J. E.; Kinloch, I. A.; Shaffer, M. S. P.; Windle, A. H. *Polymer* **2003**, *44*, 5893.

(6) Skakalova, V.; Dettlaff-Weglikowska, U.; Roth, S. *Synth. Met.* **2005**, *152*, 349.

(7) Nogales, A.; Broza, G.; Roslaniec, Z.; Schulte, K.; Sics, I.; Hsiao, B. S.; Sanz, A.; Garcia-Gutierrez, M. C.; Rueda, D. R.; Domingo, C.; Ezquerro, T. A. *Macromolecules* **2004**, *37*, 7669.

(8) Ha, M. L. P.; Grady, B. P.; Lolli, G.; Resasco, D. E.; Ford, W. T. *Macromol. Chem. Phys.* **2007**, *208*, 446.

(9) McNally, T.; Potschke, P.; Halley, P.; Murphy, M.; Martin, D.; Bell, S. E. J.; Brennan, G. P.; Bein, D.; Lemoine, P.; Quinn, J. P. *Polymer* **2005**, *46*, 8222.

(10) Seo, M.-K.; Park, S.-J. *Chem. Phys. Lett.* **2004**, *395*, 44.

(11) Coleman, J. N.; Curran, S.; Dalton, A. B.; Davey, A. P.; McCarty, B.; Blau, W.; Barklie, R. C. *Phys. Rev. B* **1998**, *58*, 7492.

(12) Du, F.; Fischer, J. E.; Winey, K. I. *J. Polym. Sci., Part B: Polym. Phys.* **2003**, *41*, 3333.

(13) Benoit, J.-M.; Corraze, B.; Lefrant, S.; Blau, W. J.; Bernier, P.; Chauvet, O. *Synth. Met.* **2001**, *121*, 1215.

(14) Kashiwagi, T.; Fagan, J.; Douglas, J. F.; Yamamoto, K.; Heckert, A. N.; Leigh, S. D.; Obrzut, J.; Du, F.; Lin-Gibson, S.; Mu, M.; Winey, K. I.; Haggenueller, R. *Polymer* **2007**, *48*, 4855.

(15) Winey, K. I.; Kashiwagi, T.; Mu, M. *MRS Bull.* **2007**, *32*, 348.

The objective of this research was to determine how SWNT of varied types can be dispersed into a typical amorphous polymer, polystyrene. We examined two methods of preparation of composites. First, we dispersed nanotubes in chloroform with the aid of poly[(*m*-phenylenevinylene)-*co*-(2,5-dioctoxy-*p*-phenylenevinylene)] (PmPV). The ability of this copolymer to form stable dispersions of SWNT in chloroform at concentrations as high as 1.2 g/L has been demonstrated by Star.<sup>16</sup> Chen<sup>17</sup> used a poly(phenylenethynylene) (PPE), a copolymer similar to PmPV in structure, to solubilize SWNT in chloroform and showed that PPE is more efficient than PmPV for the small diameter nanotubes. Ramasubramaniam<sup>4</sup> utilized PPE to prepare composites with polystyrene by spin-coating. In the present work, rotary evaporation under a vacuum was employed to remove the chloroform from the composite. Our second method of composite preparation is precipitation into water of a DMF solution of polystyrene and nanotubes that had been oxidized by nitric acid. We found previously<sup>18</sup> that sonication of nanotubes in 8 M nitric acid for 60 min significantly increases their solubility in DMF while preserving the electronic structure of nanotubes.

### Experimental Section

**Materials.** CoMoCat nanotubes in the form of a 2% aqueous gel purified by the basic (alkali) protocol<sup>19</sup> were obtained from Southwest Nanotechnologies, Inc., Norman, OK.<sup>20</sup> HiPco SWNT material in the form of a puffy fibrous powder, lot R0488, was purchased from Carbon Nanotechnologies, Inc., Houston, TX.<sup>21</sup> Laser oven SWNT (PLV) in the form of a black powder, batch JSC-338, purified by the soft-baking protocol<sup>22</sup> were obtained from NASA Johnson Space Center, Houston, TX.<sup>23</sup> PmPV was purchased from Aldrich. The  $M_n$  and  $M_w/M_n$  were 3700 g/mol and 1.4 by SEC using THF as eluant and polystyrene standards. Polystyrene of  $M_w = 2 \times 10^5$  and  $M_w/M_n = 3.6$  was the matrix polymer. All solvents were from Pharmco and Spectrum and were dried over anhydrous potassium carbonate. All other chemicals were from Sigma or Aldrich.

**Instruments and Measurements.** Ultrasonication was performed using a Fisher FS-30 160W 3QT ultrasonic cleaner or a Microson XL-2000 22 KHz ultrasonic cell disruptor. Atomic force micrographs were obtained using a Multimode Nanoscope IIIa SPM (Digital Instruments, Santa Barbara, CA) operating in the tapping mode. The samples were prepared by applying a drop of a suspension on a mica chip for a short time (10 min for DMF solutions and 10 s for  $\text{CHCl}_3$  solutions) followed by removing the excess liquid and drying in a stream of nitrogen. Electrical

conductivity was measured by a two-probe method using a Keithley 610C Electrometer. Composite samples were heated in a  $15 \times 15 \times 0.5 \text{ mm}^3$  mold to 175 °C and pressed at 10 000 psi for 1 min. The pressure was released, and the hot mold was taken out of the press to cool. Cooling the sample slowly under continued pressure made no difference in the conductivity. Pressing the samples at 140 °C resulted in lower conductivity. Two pieces of each composite were prepared. The conductivity of each piece was measured in 6 spots (3 spots on each side), resulting in 12 data points for each sample. In order to calculate the percolation threshold, eq 1 was transformed into the logarithmic form:

$$\log(\sigma) = \beta \log(m - m_c) + \log(C) \quad (2)$$

In this equation, the volume fraction of the filler is substituted by mass fraction, which still allows for direct comparison between materials. The values of  $m_c$ ,  $\beta$ , and  $C$  were calculated by linear regression analysis. Thin films ( $50 \pm 10 \mu\text{m}$ ) of the composites for microscopy and spectroscopy were pressed using the same press and conditions. Optical microscopy was performed on a Leica DM IRB optical microscope at 100 $\times$  magnification. The UV-vis-NIR spectra of the films and organic dispersions were obtained on a Cary-5000 spectrometer at 200–2000 nm. Thermogravimetric analyses were performed in air using a Shimadzu TGA50/50H instrument. Scanning electron micrographs were obtained on a JEOL JSM 6400 instrument operating at 20–30 kV accelerating voltage. The micrographs of the noncoated composite films were taken using a technique described by Loos<sup>24</sup> that allowed imaging the nanotubes located throughout an electrically conducting composite.

**Solubility of SWNT/PmPV in Chloroform.** PmPV was soluble in THF, toluene, and chloroform and poorly soluble in DMF. Only chloroform gave stable dispersions of carbon nanotubes. In this paper, we define a solution to SWNT to be a dispersion in which there are no visible solids. To estimate solubility, a stock dispersion containing 0.5 g/L SWNT and PmPV at concentrations of 0.5, 1.0, 1.5, and 2.0 g/L in chloroform were bath sonicated for 60 min and stirred for 24 h. All of the dispersions looked black. Observation through a 2 mm glass cell revealed small suspended particles. These stock dispersions were diluted with chloroform yielding a series of dispersions with concentrations of SWNT from 0.01 to 0.3 g/L and transferred to 12 mL glass vials. The vials were placed in a 20 °C water bath, tip sonicated for 15 min at 15 W, and left for 2 h, after which time the liquid was examined by eye without magnification. If no particles were observed, the solution was considered to be uniform. From some of the uniform solutions, some black sediment appeared on the bottom of the vial after 8–10 h. The sediment could be redispersed simply by shaking the vial. For solutions of SWNT where the concentration was much lower than the solubility limit, a uniform dispersion was obtained by diluting the stock dispersion and vigorous shaking for 5–6 s, whereas for SWNT concentrations close to the solubility limit sonication was always required to make the dispersion uniform. Above the solubility limits, sonication for up to 40 min did not make the dispersion uniform.

**SWNT/PmPV/PS Composites.** Typically, 1–20 mL of a stock dispersion containing 0.5 g/L SWNT and 2.0 g/L PmPV in chloroform was diluted by 1:5 and bath sonicated for 60 min. Water in the bath was replaced frequently in order to keep the temperature below 40 °C. A 40 g/L solution of polystyrene in chloroform was prepared separately. The dispersion of SWNT was mixed with the solution of polystyrene in a ratio yielding the required proportion

- (16) Star, A. J.; Stoddart, F.; Steuerman, D.; Diehl, M.; Boukai, A.; Wong, E. W.; Yang, X.; Chung, S.-W.; Choi, H.; Heath, J. R. *Angew. Chem., Int. Ed.* **2001**, *40*, 1721.
- (17) Chen, J.; Liu, H.; Weimer, W. A.; Halls, M. D.; Waldeck, D. H.; Walker, G. C. *J. Am. Chem. Soc.* **2002**, *124*, 9034.
- (18) Tchoul, M. N.; Ford, W. T.; Lolli, G.; Resasco, D. E.; Arepalli, S. *Chem. Mater.* **2007**, *19*, 5765.
- (19) Matarredona, O.; Rhoads, H.; Li, Z.; Harwell, J. H.; Balzano, L.; Resasco, D. E. *J. Phys. Chem. B* **2003**, *107*, 13357.
- (20) Kityanan, B.; Alvarez, W. E.; Harwell, J. H.; Resasco, D. E. *Chem. Phys. Lett.* **2000**, *317*, 497.
- (21) Dai, H.; Rinzler, A. G.; Nikolaev, P.; Thess, A.; Colbert, D. T.; Smalley, R. E. *Chem. Phys. Lett.* **1996**, *260*, 471.
- (22) Nikolaev, P.; Gorelik, O.; Allada, R. K.; Sosa, E.; Arepalli, S.; Yowell, L. *J. Phys. Chem. C* **2007**, *111*, 17678.
- (23) Arepalli, S.; Nikolaev, P.; Holmes, W.; Files, B. S. *Appl. Phys. Lett.* **2001**, *78*, 1610.

- (24) Loos, J.; Alexeev, A.; Grossiord, N.; Koningc, C. E.; Regev, O. *Ultramicroscopy* **2005**, *104*, 160.

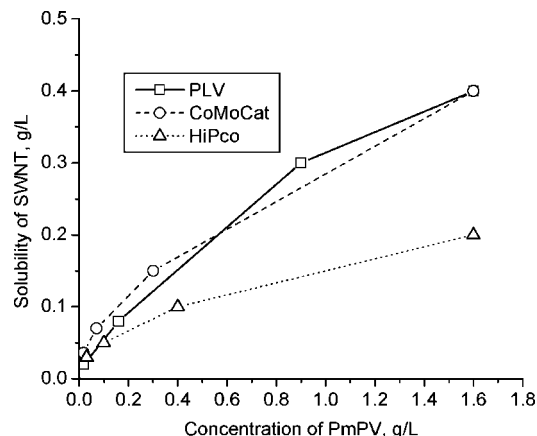


**Figure 1.** Dependence of solubility of SWNT in chloroform on concentration of PmPV.

of nanotubes and polystyrene. The mixture was stirred for 1 h followed by tip-sonication at 15 W for 15 min at room temperature. The chloroform was removed by rotary evaporation, then vacuum at 50 °C for 60 min, and finally heat at 110 °C for 1 h.

**Composites of Oxidized SWNT and Polystyrene.** The nanotubes were oxidized by bath sonication in 8 M nitric acid for 60 min followed by washing out the acid according to the previously reported procedure.<sup>18</sup> Oxidized nanotubes were dispersed in DMF at 0.5 g/L by bath sonication for 1 h and stirring for 24 h. The resulting dispersion was diluted with DMF by 1:10 and bath sonicated for 60 min. Water in the bath was replaced frequently in order to keep the temperature below 40 °C. A 20 g/L solution of polystyrene in DMF was prepared separately. The dispersion of SWNT was mixed with the solution of polystyrene in a ratio yielding the required proportion of nanotubes and polystyrene. The mixture was stirred for 1 h followed by bath sonication for 30 min. The resulting mixture was precipitated by pouring into a 10-fold volume of water vigorously mixed with a mechanical stirrer followed by filtration, washing the solid with water and methanol, and drying it at 110 °C for 1 h.

## Results and Discussion

**Composites of SWNT/PmPV/Polystyrene.** Figure 1 shows the solubility of nanotubes in chloroform in the presence of PmPV. For the concentrations of SWNT and PmPV below the lines, the dispersions were uniform, whereas for the concentrations above the lines, the dispersions had visible suspended particles. In this paper, we define soluble as having no visible particles. These dispersions were obtained by diluting a more concentrated stock dispersion. Attempts to disperse nanotubes starting with low concentrations of SWNT and PmPV failed regardless of the sonication time. We attribute this phenomenon to adsorption of PmPV on the surface of bundled SWNT. Adsorption is generally described by a Langmuir isotherm, where the surface coverage  $G_p$  (amount of solute adsorbed per unit area of adsorbent) increases with the increase of concentration of solute C in accordance with eq 3<sup>25</sup>

$$G_p = G_{ps}bC/(1 + bC), \quad (3)$$

We estimate that concentration of PmPV in chloroform of 0.5 g/L and higher is sufficient for obtaining uniform

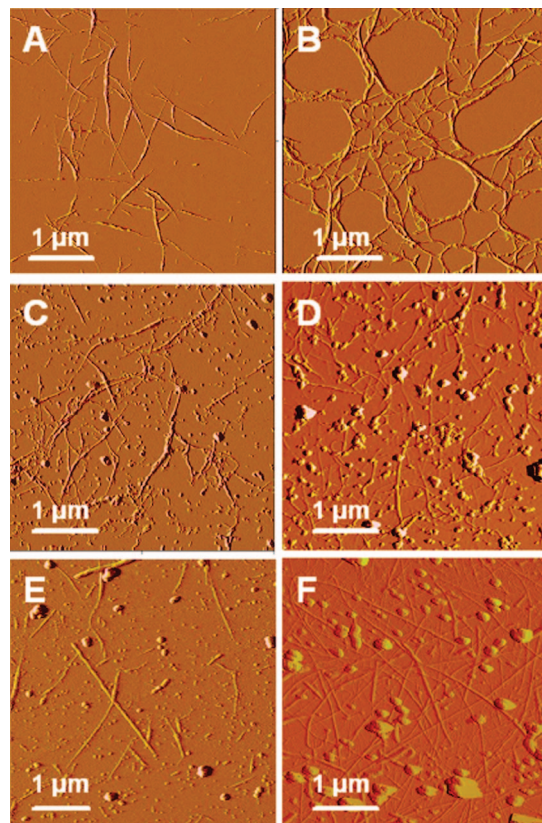


**Figure 2.** AFM of the pristine and PmPV-functionalized SWNT deposited on mica. (A, C, E) Pristine (A) HiPco, (C) CoMoCat, and (E) PLV. (B, D, F) PmPV-functionalized (B) HiPco, (D) CoMoCat, and (F) PLV.

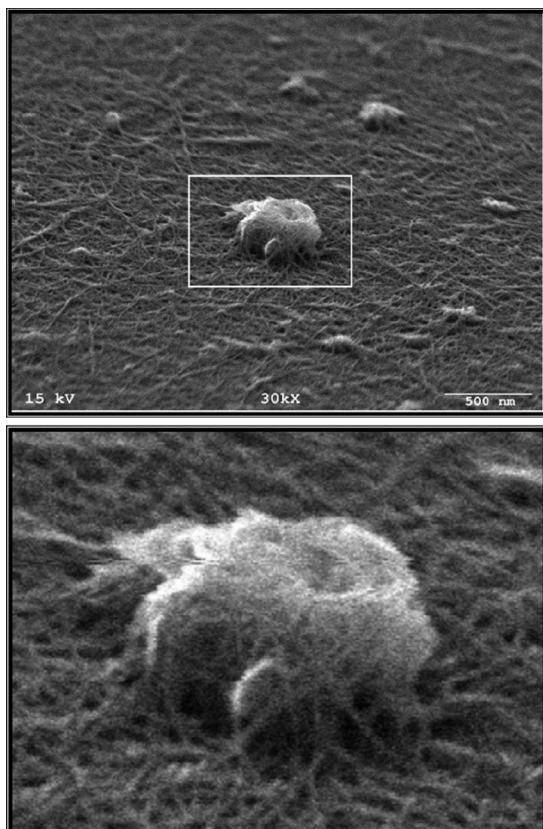
dispersions of SWNT after dilution, which indicates sufficient adsorption of the copolymer. Figure 1 shows that in order to increase concentration of nanotubes in dispersion while keeping it uniform, the ratio of PmPV to SWNT has to be increased too.

Figure 2 presents AFM micrographs of pristine and PmPV-functionalized nanotubes. In AFM section analyses of the PmPV-functionalized SWNT most of nanotubes appeared as small bundles less than 10 nm in diameter for all three types of SWNT. The AFM of HiPco SWNT shows almost entirely tubular objects. Globular particles appear on the micrographs of the CoMoCat and PLV materials in both pristine and PmPV-functionalized form. According to the manufacturer's information the PLV sample contained about 20% of amorphous carbon, which was confirmed by TGA and SEM (see the Supporting Information). TGA and SEM of the HiPco and CoMoCat SWNT (also in the Supporting Information) showed no amorphous carbon. Further investigation of the CoMoCat nanotubes by SEM revealed that the globular particles on the AFM are in fact coils of nanotubes as shown in Figure 3.

Optical microscopy images of the polystyrene composites of the PmPV-functionalized nanotubes in Figure 4 show black particles 5–20 μm in size that correspond to agglomerates of nanotubes, according to the higher-magnification SEM images.

Figure 5 presents the optical absorption spectra of the PmPV-functionalized nanotubes acquired from solutions and from solid films of composites. The spectra were normalized at 800 nm for CoMoCat, 1000 nm for HiPco, and 1300 nm

(25) Lipatov, Y. S.; Sergeeva, L. M *Adsorption of Polymers*; John Wiley and Sons: New York, 1974.



**Figure 3.** SEM of typical pristine HF-washed CoMoCat SWNT. Bottom image: zoomed area in the rectangle.

for PLV, because of absence of major interband transition peaks at these wavelengths. The sharpness of the peaks expressed as the height to width ratio is an indicator of the dispersion state of nanotubes: bundling reduces the sharpness.<sup>26</sup> The peaks from solid films look as sharp and distinct as those from solutions, which suggests that there was no significant aggregation of nanotubes during the evaporation of chloroform or during the coagulations of the dispersions in water. As the SEM images of Figure 4 suggest, the nanotubes in those aggregates are packed loosely. This loose packing should allow the individual tubes to still reveal their absorption features.

**Composites of Oxidized SWNT in Polystyrene.** Oxidized SWNT and polystyrene were precipitated from DMF into water to prepare composites. Evaporation did not work for these materials; the slow evaporation of the DMF resulted in premature aggregation of nanotubes as the solution concentrated. Figure 6 presents AFM of the oxidized nanotubes deposited from DMF dispersions. In section analyses of the AFM images over 80% of tubular objects had heights 10 nm and less, but the average diameter was greater than that in the PmPV-functionalized samples. Small globular particles appearing on the AFM image of HiPco tubes in Figure 6A compared to the pristine sample in Figure 2A, and some increase in number of these particles for the oxidized CoMoCat sample, suggest accumulation of amorphous carbon after the oxidation procedure. The oxidized SWNT were moderately shorter than the PmPV dispersed

materials that were subjected only to a brief sonication. Optical micrographs of the composites of oxidized SWNT in Figure 6 look very similar to those for the PmPV-functionalized composites: small tubular particles in HiPco composites and large globular agglomerates in CoMoCat and PLV composites. HiPco material had fewer large agglomerates regardless of the way the composite was prepared.

Optical absorption spectra of the DMF dispersions and coagulated solid composites in Figure 5D–F, similarly to the PmPV-functionalized material, did not show a decrease in the interband transition peaks intensities, which is an indicator that the coagulation did not occur with a noticeable bundling of nanotubes. According to Itkis,<sup>27</sup> amorphous carbon accumulated in the material should decrease the relative area under the peaks, which was not the case for our slightly oxidized material, as judged by the UV–vis spectra.

**Electrical Conductivity of the SWNT Composites.** Figure 7 reports electrical conductivity of the polystyrene composites of the PmPV-functionalized nanotubes, and Figure 8 reports the conductivity data for the composites of oxidized nanotubes. The results for the percolation threshold and critical exponent  $\beta$  of eq 2 are displayed in Table 1. The graphs used to calculate the percolation thresholds are in the Supporting Information. The values for the percolation threshold are comparable to the values of 0.045–0.3% reported in literature for other composites of SWNT and polystyrene.<sup>4,8,12,28,29</sup> Table 1 also reports the diameters ( $d$ ) and lengths ( $L$ ) of nanotubes obtained from AFM and the aspect ratios  $L/d$ . The most important general result is that despite using three different types of SWNT and two different methods of dispersion, the percolation thresholds of conductivity, the plateau conductivities, and the lengths and diameters of tube bundles are remarkably similar.

From the data in Table 1 and Figures 7 and 8, three observations are significant. (1) The values for the percolation threshold were 0.17–0.3% for the PmPV-functionalized SWNT composites and 0.4–0.5% for the oxidized SWNT composites. According to theory, the percolation threshold in a system of conducting cylinders depends upon the aspect ratio of the cylinders.<sup>30</sup> The oxidized nanotubes have a smaller aspect ratio than the PmPV dispersed materials. Consequently, composites containing oxidized SWNT would be expected to have the higher percolation threshold. (2) The CoMoCat composites have higher percolation thresholds than the HiPco and the PLV composites. (3) The plateau conductivity at  $>1$  wt % nanotubes is highest for the HiPco composites. Possible reasons for the higher percolation thresholds of CoMoCat composites and the higher plateau conductivity of HiPco composites are discussed next.

Some of the differences between HiPco, CoMoCat, and PLV SWNT that might affect electrical conductivity of the composites are as follows. (1) The resistances at bundle-to-

(27) Itkis, M. E.; Perea, D. E.; Niyogi, S.; Rickard, S. M.; Hamon, M. A.; Hu, H.; Zhao, B.; Haddon, R. C. *Nano Lett.* **2003**, *3*, 309.

(28) Chang, T.-E.; Kisluk, A.; Rhodes, S. M.; Brittain, W. J.; Sokolov, A. P. *Polymer* **2006**, *47*, 7740.

(29) Grossiord, N.; Miltner, H. E.; Loos, J.; Meuldijk, J.; Van Mele, B.; Koning, C. E. *Chem. Mater.* **2007**, *19*, 3787.

(30) Munson-McGee, S. H. *Phys. Rev. B* **1991**, *43*, 3331.

(26) Reich, S.; Thomsen, C.; Ordejón, P. *Phys. Rev. B* **2002**, *65*, 155411/1.

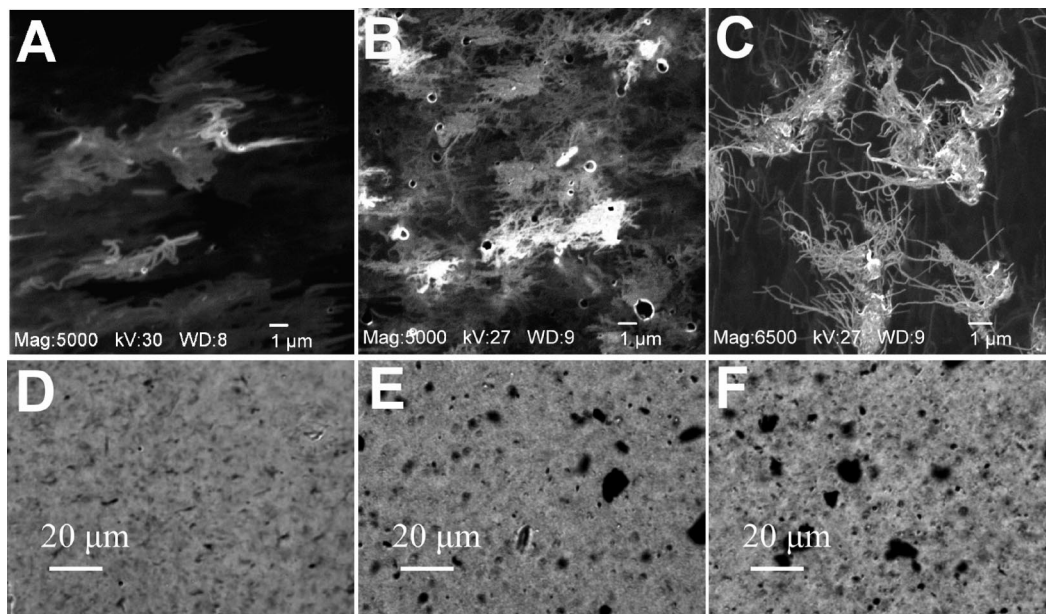


**Figure 4.** (A–C) Scanning electron microscopy and (D–F) optical microscopy images of pressed films of SWNT–PmPV–PS composites made from (A, D) HiPco, (B, E) CoMoCat, and (C, F) PLV nanotubes.

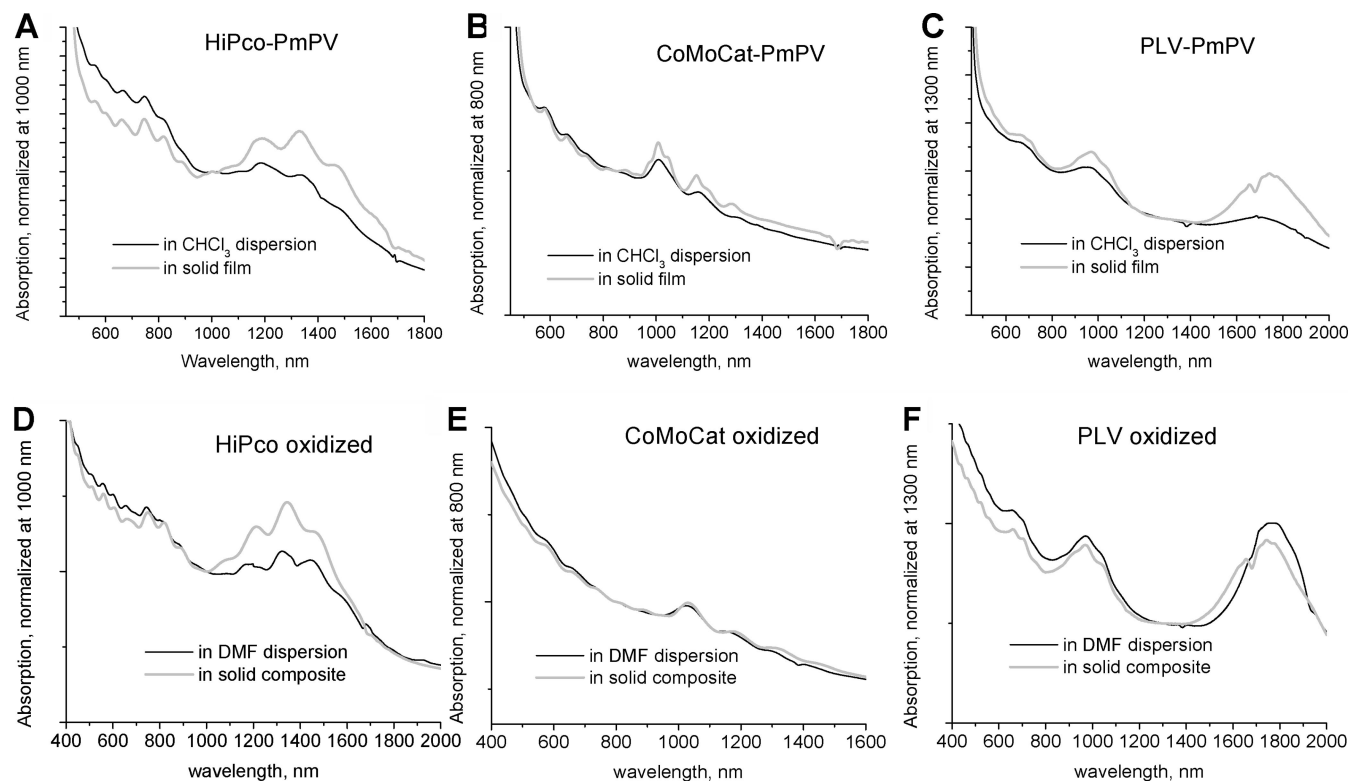


**Figure 5.** Optical absorption of the (A–C) PmPV-functionalized and (D–F) oxidized SWNT in chloroform dispersions and in solid polystyrene composites. (A, D) HiPco, (B, E) CoMoCat, (C, F) PLV.

bundle contacts may differ. We have measured only bulk conductivities, not conductivities of nanoscopic tube bundles. (2) The densities of the nanotube bundles may differ. The average diameter of individual nanotubes is 0.8 nm for CoMoCat,<sup>31</sup> 1.0 nm for HiPco,<sup>32</sup> and 1.3 for PLV.<sup>33</sup>

The smaller is the diameter, the greater the density of an individual nanotube or a tightly packed bundle of nanotubes because of the smaller void volume inside the tube. However, the greatest differences in density are likely due to imperfect packing, which lowers the density, and catalyst residue, which increases the density. Higher density means a smaller volume fraction for a given weight of nanotubes. The den-

(31) Bachilo, S. M.; Balzano, L.; Herrera, J. E.; Pompeo, F.; Resasco, D. E.; Weisman, R. B. *J. Am. Chem. Soc.* **2003**, *125*, 11186.

(32) Zhou, W.; Ooi, Y. H.; Russo, R.; Papanek, P.; Luzzi, D. E.; Fischer, J. E.; Bronikowski, M. J.; Willis, P. A.; Smalley, R. E. *Chem. Phys. Lett.* **2001**, *350*, 6.

(33) Yudasaka, M.; Sensui, N.; Takizawa, M.; Bandow, S.; Ichihashi, T.; Iijima, S. *Chem. Phys. Lett.* **1999**, *312*, 155.

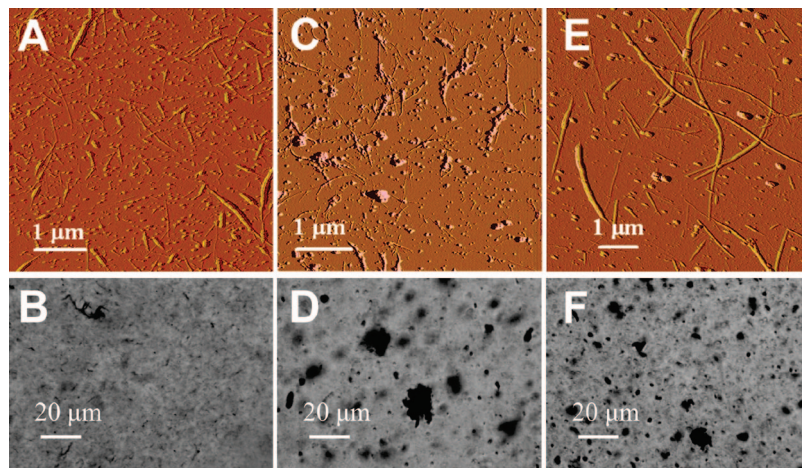


**Figure 6.** AFM of the oxidized SWCNT and optical micrographs of the 0.6% oxidized SWCNT in polystyrene. (A, B) HiPco; (C, D) CoMoCat; (E, F) PLV.

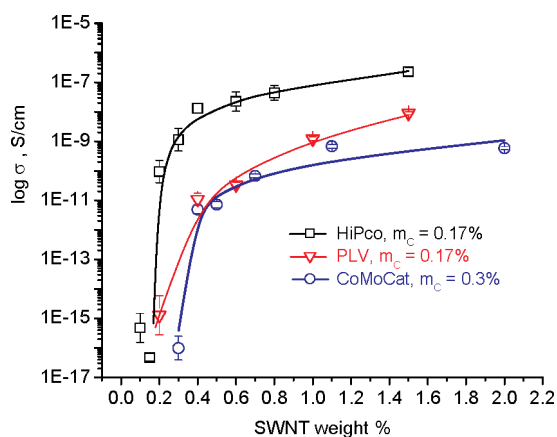


**Figure 7.** Electrical conductivity of the composites of SWCNT dispersed by PmPV in polystyrene. Error bars are two standard deviations.

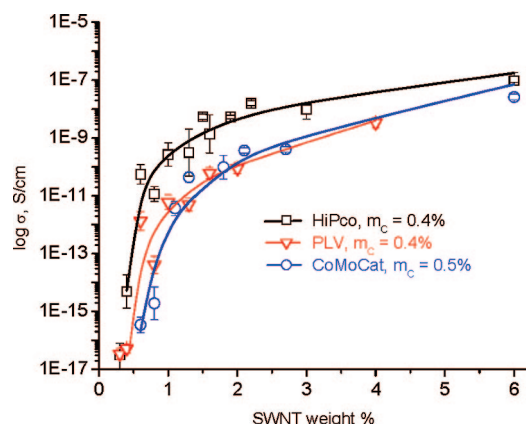


**Figure 8.** Electrical conductivity of oxidized SWCNT in polystyrene. Error bars are two standard deviations.

sities of the nanotube bundles in our polystyrene composites have not been measured. (3) The amounts and types of impurities in the various nanotubes differ. According to the suppliers, HiPco SWCNT contain about 20% catalyst residue and little amorphous carbon, PLV SWCNT contain about 6% catalyst residue and 20% amorphous carbon, and CoMoCat SWCNT contain about 8% catalyst residue and little amorphous carbon. TGA data in the Supporting Information verify these reports of impurities by the suppliers. The nitric acid

**Table 1.** Sizes of Nanotubes and Calculated Parameters from eq 2

SWNT	average diameter $d$ (nm)	average length $L$ (nm)	aspect ratio $L/d$	percolation threshold $m_c$ (wt %)	critical exponent $\beta$
HiPco–PmPV	3.2	734	230	0.17	2.0
HiPco oxidized	4.4	540	122	0.4	2.9
CoMoCat–PmPV	3.1	690	223	0.3	2.0
CoMoCat oxidized	4.2	620	148	0.5	4.8
PLV–PmPV	4.6	1020	222	0.17	4.1
PLV oxidized	5.8	790	136	0.4	4.5

oxidation procedure reduces the amounts of catalyst impurities to 10% in HiPco, 5% in PLV, and 6% in CoMoCat SWNT.<sup>18</sup> If a bundle of nanotubes has metallic conductivity already, the presence of metal catalyst particles will affect the conductivity greatly only if the particles reduce contact resistance. (4) The content of metallic vs semiconducting tubes differs greatly by tube type. From the distributions of the  $(n, m)$  species the CoMoCat SWCNT were estimated to be 9% metallic,<sup>34</sup> and the HiPco SWCNT contain approximately 20% of metallic nanotubes.<sup>35</sup> Because of the low metallic tube content and the size distributions of bundles, a significant fraction of the CoMoCat bundles should be semiconducting rather than metallic. Although the percolation threshold relates to the geometry of the nanotube bundles and contact resistances, the conductivity of the composites at the plateau region in Figures 7 and 8 may depend upon the conductivity of the nanotube material itself. From conductivity measurements of individual tubes and bundles, Skakalova<sup>36</sup> confirmed that the metallic tubes carry most of the current in SWCNT networks, and that the resistance is dominated by semiconducting SWNT. Hence composites made from CoMoCat tubes would be expected to have lower conductivity in the plateau region than composites made from HiPco tubes.

(34) Jorio, A.; Santos, A. P.; Ribeiro, H. B.; Fantini, C.; Souza, M.; Vieira, J. P. M.; Furtado, C. A.; Jiang, J.; Saito, R.; Balzano, L.; Resasco, D. E.; Pimenta, M. A. *Phys. Rev. B* **2005**, *72*, 075207/1.

(35) Jorio, A.; Fantini, C.; Pimenta, M. A.; Capaz, R. B.; Samsonidze, G. G.; Dresselhaus, G.; Dresselhaus, M. S.; Jiang, J.; Kobayashi, N.; Gruneis, A.; Saito, R. *Phys. Rev. B* **2005**, *71*, 075401.

(36) Skakalova, V.; Kaiser, A. B.; Woo, Y. S.; Roth, S. *Phys. Rev. B* **2006**, *74*, 085403.

### Conclusions

PmPV is a good stabilizing agent for dispersions of carbon nanotubes, enabling preparation of polystyrene composites via rapid evaporation of chloroform from dispersions of SWNT in polystyrene solution. However, the presence of PmPV may detract from the mechanical properties of the composite. The use of oxidized SWNT and no extra polymer or surfactant simplifies the composite content. The nitric acid treatment shortens the nanotubes, decreasing the aspect ratio compared with the PmPV dispersed nanotubes. The smaller aspect ratio nanotube bundles in polystyrene composites have a higher percolation threshold of electrical conductivity, which is consistent with percolation theory. The electrical conductivity in the plateau region above the percolation threshold depends on the type of SWNT material, which could be attributed to the differences in the fraction of metallic nanotubes.

**Acknowledgment.** We thank Professor Jay Hannan of the School of Mechanical and Aerospace Engineering at Oklahoma State University for use of the hydraulic press and Professor LeGrande Slaughter of the Department of Chemistry at Oklahoma State University for use of the TGA instrument. The CoMoCat material was provided by Southwest Nanotechnologies, Inc., Norman, OK. The PLV material was provided by NASA Johnson Space Center. Financial support from the Oklahoma State Regents for Higher Education, NSF EPSCoR, and NASA Grant NNJ05H105C is greatly appreciated.

**Supporting Information Available:** SEM and TGA of the pristine SWNT materials used in this work; AFM micrographs; length and height distributions of SWNT on AFM micrographs; and graphical determinations of thresholds of electrical conductivity (PDF). This information is available free of charge via the Internet at <http://pubs.acs.org>.

CM703625W